

Electronic supplementary information

In Situ Fabrication of Defect Engineering in Multifunctional Layer with Strong Zincophilicity and High Zn-Ion Conductivity on Zn Anodes

Maoni Lu, ‡^{ab} Daochuan Jiang, ‡^a Xiaoxing Zhou, ^{ab} Sichen Li, ^{ab} Xinghao Li, ^{ab} Ping Chen, ^a Zhenjie Sun, ^{*a} Junnan Hao, ^{*c} Manzhou Zhu, ^{ab} and Peng Li^{*ab}

^a Department of Chemistry and Center for Atomic Engineering of Advanced Materials, School of Materials Science and Engineering, Anhui University, Hefei 230601, P. R. China

^b Key Laboratory of Structure and Functional Regulation of Hybrid Materials, Ministry of Education, Anhui University, Hefei 230601, P. R. China

^c School of Chemical Engineering & Advanced Materials, The University of Adelaide, Adelaide, South Australia 5005, Australia

‡ These authors contributed equally to this work.

* E-mail: sunzhenjie2008@126.com (Z. Sun), junnan.hao@adelaide.edu.au (J. Hao), peng-li@ahu.edu.cn (P. Li).

Experiment section

Materials

ZnSO₄·7H₂O (99%), iodine (I₂, 99.99%) and N-methyl-2-pyrrolidone (NMP, 99.5%) were bought from Aladdin (Shanghai, China). Isopropanol (AR), hydrogen peroxide (H₂O₂, 30%) and potassium permanganate (KMnO₄, AR) were obtained from Sinopharm (Shanghai, China). 2-methylimidazole (98%) was supplied by Macklin. Poly (1,1-difluoroethylene) (PVDF), super P, activated carbon (AC), Zn foil (0.10 mm), Ti foil (0.02 mm) and Cu foil (0.01 mm) were procured from Kejing Star Technology (Shenzhen, China).

Preparation of Zn@DZ-MOF electrodes

Zn@DZ-MOF anodes were fabricated by a two-step reaction process. First, one side of the Zn foil (0.10 mm) was covered with Kapton tape to protect it from oxidation. Then, the covered Zn foil was sonicated in isopropanol solvent for 30 min and then immersed in 20 mL KMnO₄ solution (0.02 M) at 85 °C for 30 min. Subsequently, the obtained Zn foil was washed and infiltrated into 20 mL 2-methylimidazole solution (0.50 M) for 48 h. The products were washed with deionized water (DI), dried at 50 °C for 24 h and cut into circular disks with a diameter of 12 mm to obtain Zn@DZ-MOF electrodes.

Preparation of zinc-based metal-organic framework (Zn@Z-MOF) electrodes

Similarly, Zn@Z-MOF anodes were synthesized using the same procedures, except that the treatment of Zn foil in 20 mL KMnO₄ solution (0.02 M) at 85 °C for 30 min was replaced with 20 mL H₂O₂ solution (30%) at 70 °C for 30 min.

Preparation of I₂-AC electrode materials

The I₂-AC cathode material was prepared by an I₂ sublimation method.¹ In general, 1.0 g of I₂ and 1.0 g of AC were completely mixed, and then placed in a hydrothermal reactor and heated at 90 °C for 4 h. The I₂-AC composite cathode material was finally obtained after the product cooling to ambient temperature.

Materials characterization

The samples were characterized by the X-ray diffraction (XRD, Smart Lab, 9 KW) analysis with Cu-Kα

radiation source in the 2θ range of $5^\circ\sim 90^\circ$. The scanning electron microscopy (SEM, Hitachi, S-4800), transmission electron microscopy (TEM, JEOL JEM-2010) and energy dispersive spectroscopy (EDS, INCA) investigations were employed to study the morphology, microstructure, and element distribution of the materials. The X-ray photoelectron spectroscopy (XPS, Thermo ESCALAB 250) analysis was recorded to characterize the surface composition. The X-ray absorption fine structure (XAFS) measurements of Mn K-edge were conducted on a TableXAFS-500 (Speccreation Instruments Co., Ltd., China). The wettability of the 2.0 M ZnSO_4 electrolyte to bare Zn, Zn@Z-MOF and Zn@DZ-MOF electrodes were investigated using a contact Angle meter (DSA30). The structural composition of the samples was collected by Fourier transformation infrared (FTIR, Bruker Tensor 27). The I_2 content in I_2 -AC was measured by the thermogravimetric analysis (TGA, Hitachi, STA200). The surface morphologies of electrodes during electrochemical deposition were observed by an electron microscope (Shenhong).

Electrochemical measurements

All full and half batteries were assembled into CR-2025 coin cells using a Glass fiber (Whatman GF/D) separator and an electrolyte of 2.0 M ZnSO_4 aqueous solution (80 μL). The cathodes were fabricated by mixing I_2 -AC powder, Super P and poly (1,1-difluoroethylene) (PVDF) in a weight ratio of 8: 1: 1 using N-methyl-2-pyrrolidone (NMP) as blending solvent. Then, the resultant slurry was coated on Ti foils and dried in a vacuum oven at 60 $^\circ\text{C}$ for 12 h. Galvanostatic Charge-Discharge (GCD) tests were carried out using a Neware Battery Test System (CT-4008T). Electrochemical impedance spectroscopy (EIS), corrosion current density, linear sweep voltammetry (LSV) and chronoamperometry (CA) were measured in a CHI 760E electrochemical workstation. Corrosion current density was tested using a three-electrode system with bare Zn, Zn@Z-MOF or Zn@DZ-MOF electrodes as working electrodes, Zn foil as the counter electrode and Ag/AgCl electrode as the reference electrode. CA was tested in symmetric batteries, LSV was conducted at 0.5 mV s^{-1} and EIS was performed in a frequency range from 0.01 Hz to 100 kHz. Zn//Cu asymmetric batteries were assembled to measure CE using commercial Cu foil as a cathode and bare Zn, Zn@Z-MOF or Zn@DZ-MOF as anodes, respectively.

Density functional theory (DFT) calculation

All calculations were conducted by using the DFT method within the Vienna Ab initio Simulation Package (VASP).² The ion-electron interactions were depicted by implementing the projector augmented wave (PAW) basis at a cutoff energy of 500 eV.³ In addition, the Perdew-Burke-Ernzerhof

(PBE) functional was employed to handle the exchange and correlation interaction within the generalized gradient approximation (GGA).⁴ A vacuum buffer of 15 Å was utilized to prevent the interaction between adjacent images. The convergence criteria of energy and force were set at 10^{-6} eV and 0.03 eV \AA^{-1} , respectively, to guarantee the thorough relaxation of all atomic positions. Empirical DFT-D3 corrections were used to treat long-range van der Waals (vdW) interactions for Z-MOF and DZ-MOF. A supercell containing $4 \times 4 \times 4$ unit cells was adopted to model the Zn (001) surface, and the bottom two layers were fixed. The first Brillouin zone was sampled with k-point meshes of $1 \times 1 \times 1$ and $3 \times 3 \times 1$ for the surface of Z-MOF and Zn (001), respectively. The binding energies of Zn (E_b) on each model were defined as follows:

$$E_b = E_{total} - E_{surf} - E_{Zn} \quad (1)$$

where E_{total} , E_{surf} and E_{Zn} are the energies of the system, the surface and the Zn atom, respectively.

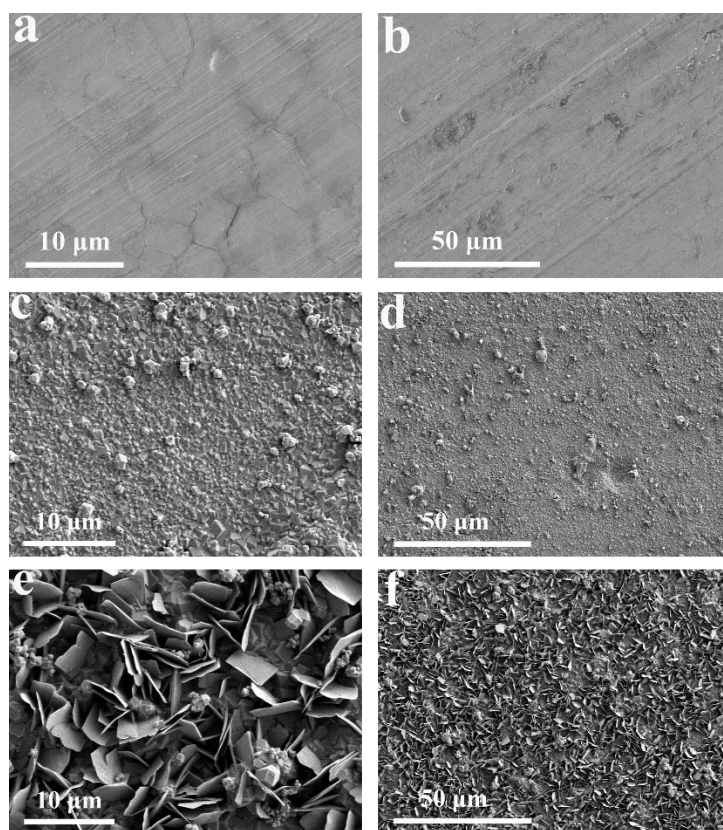


Fig. S1 SEM images of (a-b) bare Zn, (c-d) Zn@Z-MOF and (e-f) Zn@DZ-MOF electrodes.

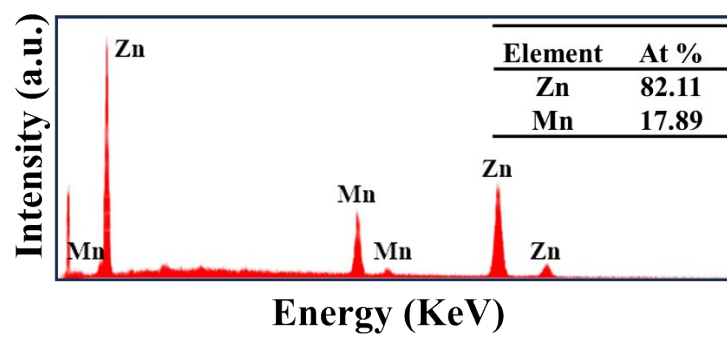


Fig. S2 EDS spectrum of the Zn@DZ-MOF electrode.

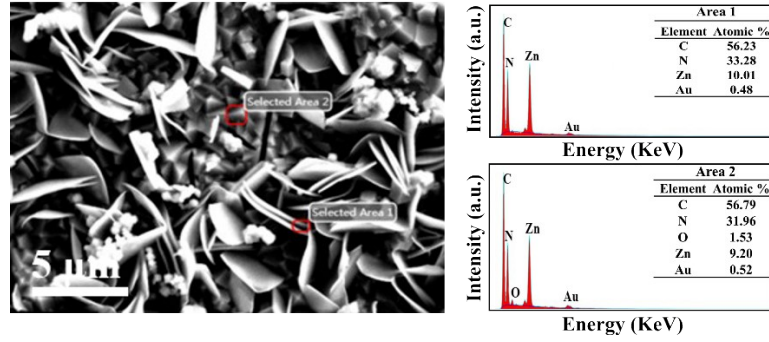


Fig. S3 SEM image of the Zn@DZ-MOF electrode and the corresponding EDS spectra at different areas.

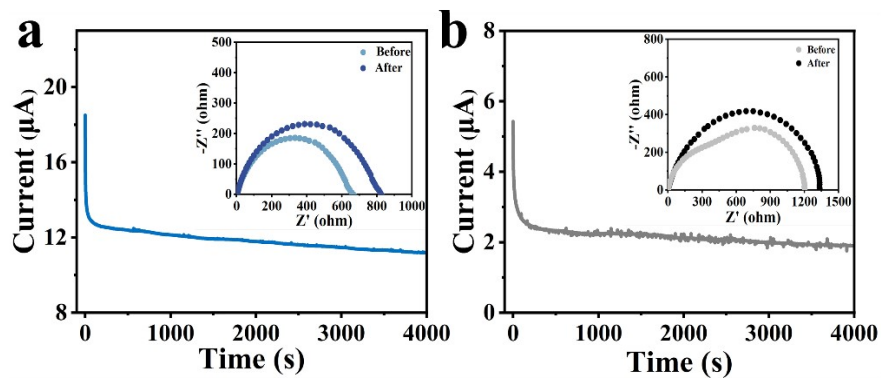


Fig. S4 Current-time curves of (a) Zn@Z-MOF//Zn@Z-MOF and (b) bare Zn//Zn symmetric batteries with an experimental potential of 20 mV. Inset: the EIS curves of symmetric batteries before and after current-time tests.

The Zn^{2+} transference number is calculated according to the Bruce-Vincent formula:

$$t_{Zn^{2+}} = \frac{I_s(\Delta V - I_0 R_0)}{I_0(\Delta V - I_s R_s)}$$

Where ΔV is the applied constant potential (20 mV), I_0 and R_0 are the incipient current and resistance of the symmetric battery, and I_s and R_s are the stable current and resistance, respectively.

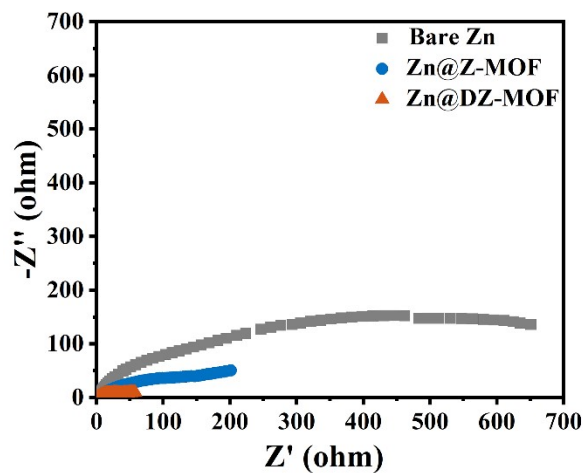


Fig. S5 EIS spectra of bare Zn//Zn, Zn@Z-MOF//Zn@Z-MOF and Zn@DZ-MOF//Zn@DZ-MOF batteries after 50 cycles.

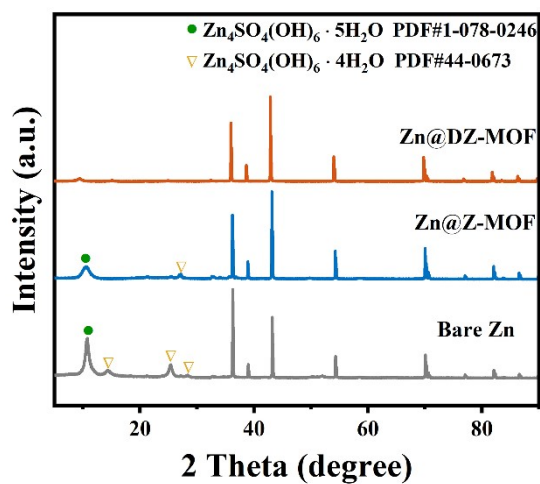


Fig. S6 XRD patterns of bare Zn, Zn@Z-MOF and Zn@DZ-MOF electrodes after immersing in 2.0 M ZnSO_4 electrolyte for 7 days.

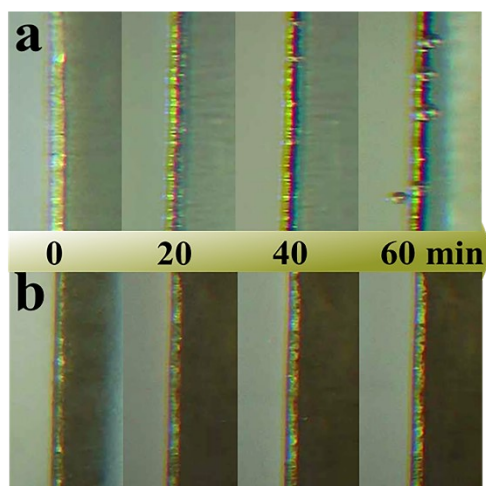


Fig. S7 In-situ optical microscopic observation of (a) bare Zn and (b) Zn@DZ-MOF electrodes at 1 mA cm⁻².

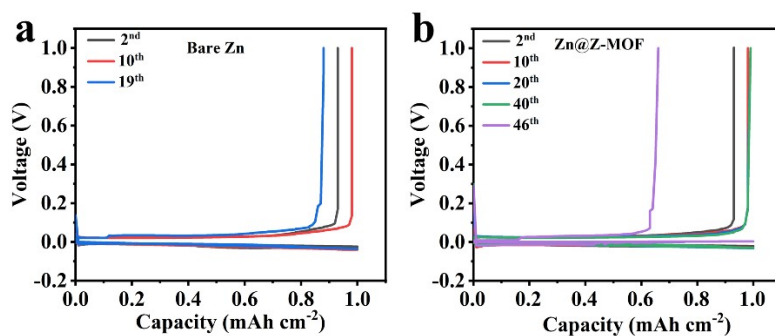


Fig. S8 Voltage profiles of (a) bare Zn//Cu and (b) Zn@Z-MOF//Cu asymmetric batteries at different cycles.

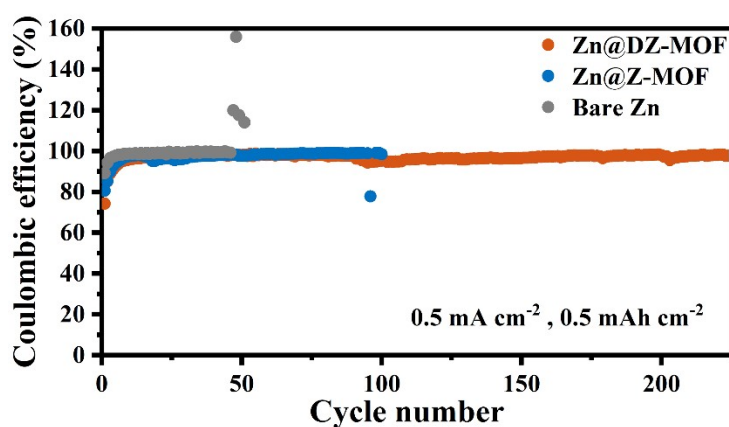


Fig. S9 Coulombic efficiencies (CEs) of Zn plating/stripping of bare Zn//Cu, Zn@Z-MOF//Cu and Zn@DZ-MOF//Cu batteries at 0.5 mA cm⁻², 0.5 mAh cm⁻².

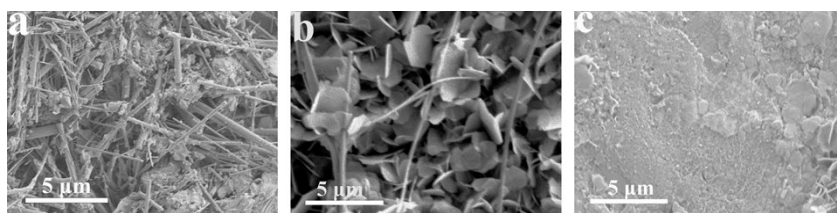


Fig. S10 SEM images of (a) bare Zn//Zn, (b) Zn@Z-MOF//Zn@Z-MOF and (c) Zn@DZ-MOF//Zn@DZ-MOF symmetric batteries after 100 cycles.

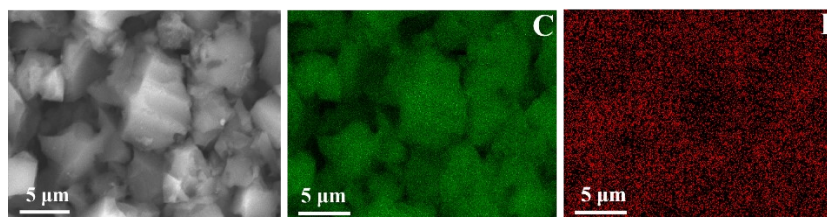


Fig. S11 SEM image and the corresponding elemental mapping of the as-prepared I₂-AC composite.

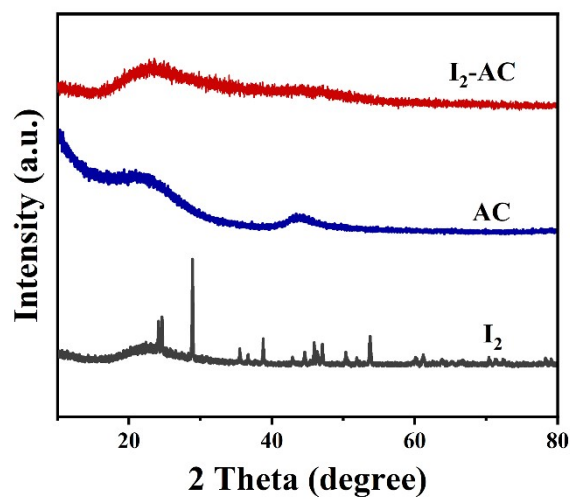


Fig. S12 XRD patterns of I₂, AC and I₂-AC.

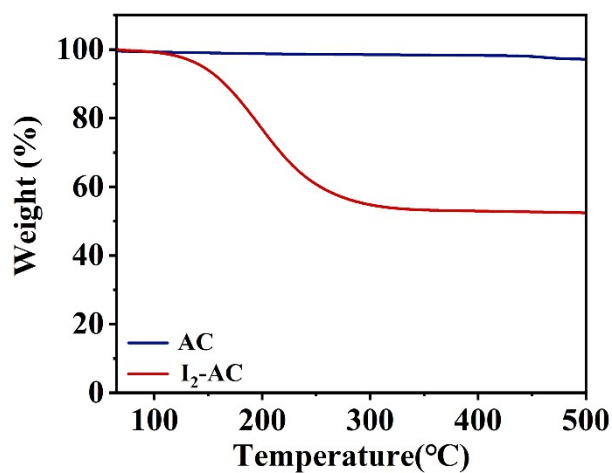


Fig. S13 TGA curves of AC and I₂-AC.

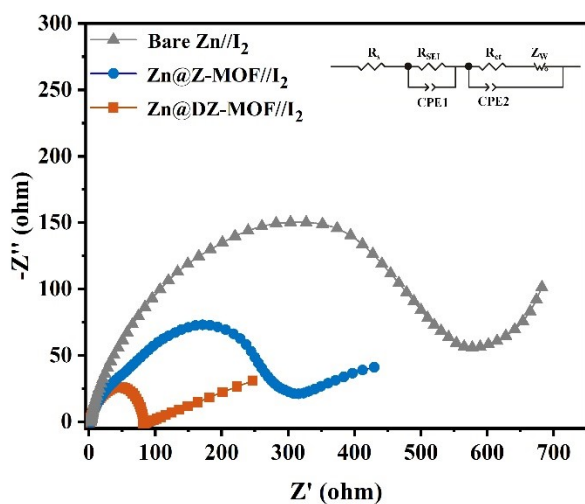


Fig. S14 The EIS spectra of bare Zn//I₂, Zn@Z-MOF//I₂ and Zn@DZ-MOF//I₂ batteries. Inset: Equivalent circuit model used for EIS fitting analysis. (R_s : electrolyte resistance; R_{ct} : charge transfer resistance; R_{SEI} : solid electrolyte interphase resistance; CPE: double-layer capacitance; Z_w : ion diffusion in the host material).

Table S1 The calculation of transference number of Zn²⁺.

electrode	I_0 (μ A)	I_s (μ A)	R_0 (Ω)	R_s (Ω)	ΔV (V)	$t_{Zn^{2+}}$
Bare Zn	5.43	1.904	1214	1324	0.02	0.269
Zn@Z-MOF	18.51	11.26	646.7	796.5	0.02	0.443
Zn@DZ-MOF	21.3	15.61	389.6	519	0.02	0.721

Table S2 Comparison of the electrochemical performance of the Zn@DZ-MOF anode with recently reported Zn-based anodes.

Protective layers	Current density	Capacity	Time (h)	Reference
	(mA cm ⁻²)	(mAh cm ⁻²)		
Zn@ZIF8	0.5	0.2	500	5
Zn@ZIF	2	1	1200	6
	2	2	700	
ZIF-8/Zn	2	2	800	7
	5	5	800	
Zn@ZIF-L	0.25	0.25	800	8
S/MX@ZnS@Zn	0.5	0.5	1600	9
	1	1	1100	
ZPS@Zn	1	1	2200	10
	5	2.5	650	
Zn-ATMP@Zn	1	1	1850	11
ZnO:S@Zn	1	1	1400	12
ZnSe@Zn	1	1	1530	13
ZnS@Zn	2	2	1100	14
SiO ₂ @Zn	1	0.5	1000	15
CeO ₂ @Zn	0.5	0.25	1300	16
Zn@ZnF ₂	0.5	1	500	17

AZ-Zn	1	1	1800	18
ZnF ₂ @Zn	0.5	0.5	715	19
Zn@PAQ	1	1	1750	20
ZIF-11	1	0.5	400	21
Sn@Zn-IP	2	1	700	22
ZCS@Zn	2	4	1200	23
ZrO ₂ @Zn	0.25	0.125	2800	24
UIO-66	3	0.5	500	25
ZnO@Zn	5	1.25	500	26
PA-Zn	2	1	1500	27
Zn@DZ-MOF	1	1	2650	This work
	2	2	1760	This work
	5	5	580	This work

Table S3 Fitting data of EIS spectra of bare Zn//I₂, Zn@Z-MOF//I₂ and Zn@DZ-MOF//I₂ batteries.

Samples	R _s (Ω)	R _{SEI} (Ω)	R _{ct} (Ω)
Bare Zn	1.712	41.8	511.2
Zn@Z-MOF	2.745	48.59	238.8
Zn@DZ-MOF	1.719	17.36	62.77

References

- 1 W. Shang, Q. Li, F. Jiang, B. Huang, J. Song, S. Yun, X. Liu, H. Kimura, J. Liu and L. Kang, *Nano-Micro Lett.*, 2022, **14**, 82.
- 2 G. Kresse and J. Furthmüller, *Comput. Mater. Sci.*, 1996, **6**, 15-50.
- 3 G. Kresse and D. Joubert, *Phys. Rev. B*, 1999, **59**, 1758-1775.
- 4 J. P. Perdew, K. Burke and M. Ernzerhof, *Phys. Rev. Lett.*, 1996, **77**, 3865-3868.
- 5 M. Cui, B. Yan, F. Mo, X. Wang, Y. Huang, J. Fan, C. Zhi and H. Li, *Chem. Eng. J.*, 2022, **434**, 13469.
- 6 X. Liu, F. Yang, W. Xu, Y. Zeng, J. He and X. Lu, *Adv. Sci.*, 2020, **7**, 2002173.
- 7 Y. Long, X. Huang, Y. Li, M. Yi, J. Hou, X. Zhou, Q. Hu, Q. Zheng and D. Lin, *J. Colloid Interf. Sci.*, 2022, **614**, 205-213.
- 8 W. He, T. Gu, X. Xu, S. Zuo, J. Shen, J. Liu and M. Zhu, *ACS Appl. Mater. Interfaces*, 2022, **14**, 40031-

40042.

- 9 Y. An, Y. Tian, C. Liu, S. Xiong, J. Feng and Y. Qian, *ACS Nano*, 2021, **15**, 15259-15273.
- 10 Y. Zhang, C. Peng, Y. Zhang, S. Yang, Z. Zeng, X. Zhang, L. Qie, L.-L. Zhang and Z. Wang, *Chem. Eng. J.*, 2022, **448**, 137653.
- 11 Z. Wang, H. Chen, H. Wang, W. Huang, H. Li and F. Pan, *ACS Energy Lett.*, 2022, **7**, 4168-4176.
- 12 D. Zhu, Y. Zheng, Y. Xiong, C. Cui, F. Ren and Y. Liu, *J. Alloys Compd.*, 2022, **918**, 165486.
- 13 X. Yang, C. Li, Z. Sun, S. Yang, Z. Shi, R. Huang, B. Liu, S. Li, Y. Wu, M. Wang, Y. Su, S. Dou and J. Sun, *Adv. Mater.*, 2021, **33**, e2105951.
- 14 W. Guo, Z. Cong, Z. Guo, C. Chang, X. Liang, Y. Liu, W. Hu and X. Pu, *Energy Storage Mater.*, 2020, **30**, 104-112.
- 15 X. Han, H. Leng, Y. Qi, P. Yang, J. Qiu, B. Zheng, J. Wu, S. Li and F. Huo, *Chem. Eng. J.*, 2022, **431**, 133931.
- 16 H. Liu, J. G. Wang, W. Hua, H. Sun, Y. Huyan, S. Tian, Z. Hou, J. Yang, C. Wei and F. Kang, *Adv. Sci.*, 2021, **8**, 2102612.
- 17 Y. Yang, C. Liu, Z. Lv, H. Yang, Y. Zhang, M. Ye, L. Chen, J. Zhao and C. C. Li, *Adv. Mater.*, 2021, **33**, 2007388.
- 18 J. Ren, C. Li, P. Li, S. Liu and L. Wang, *Chem. Eng. J.*, 2023, **462**, 142270.
- 19 J. Han, H. Euchner, M. Kuenzel, S. M. Hosseini, A. Groß, A. Varzi and S. Passerini, *ACS Energy Lett.*, 2021, **6**, 3063-3071.
- 20 D. Xie, Z. W. Wang, Z. Y. Gu, W. Y. Diao, F. Y. Tao, C. Liu, H. Z. Sun, X. L. Wu, J. W. Wang and J. P. Zhang, *Adv. Funct. Mater.*, 2022, **32**, 2204066.
- 21 21. M. He, C. Shu, A. Hu, R. Zheng, M. Li, Z. Ran and J. Long, *Energy Storage Mater.*, 2022, **44**, 452-460.
- 22 Q. Cao, Z. Pan, Y. Gao, J. Pu, G. Fu, G. Cheng and C. Guan, *Adv. Funct. Mater.*, 2022, **32**, 2205771.
- 23 Y. Chu, S. Zhang, S. Wu, Z. Hu, G. Cui and J. Luo, *Energy Environ. Sci.*, 2021, **14**, 3609-3620.
- 24 P. Liang, J. Yi, X. Liu, K. Wu, Z. Wang, J. Cui, Y. Liu, Y. Wang, Y. Xia and J. Zhang, *Adv. Funct. Mater.*, 2020, **30**, 1908528.
- 25 M. Liu, L. Yang, H. Liu, A. Amine, Q. Zhao, Y. Song, J. Yang, K. Wang and F. Pan, *ACS Appl. Mater. Interfaces*, 2019, **11**, 32046-32051.
- 26 X. Xie, S. Liang, J. Gao, S. Guo, J. Guo, C. Wang, G. Xu, X. Wu, G. Chen and J. Zhou, *Energy Environ. Sci.*, 2020, **13**, 503-510.
- 27 Y. Zhang, C. Peng, Z. Zeng, X. Zhang, L. Zhang, Y. Ma and Z. Wang, *ACS Appl. Mater. Interfaces*, 2022, **14**, 10419-10427.